

Comparison of Ring Current Methods for Use in Molecular Modeling Refinement of NMR Derived Three-Dimensional Structures

Guillermo Moyna,[†] Randy J. Zauhar,[‡] Howard J. Williams,[†] Ronald J. Nachman,[§] and A. I. Scott^{*,†}

Center for Biological NMR, Department of Chemistry, Texas A&M University, P. O. Box 300012, College Station, Texas 77842-3012, Tripos Associates, Inc., 1699 S. Hanley Road, St. Louis, Missouri 63144-2913, and Veterinary Entomology Research Unit, FAPRL, Agricultural Research Service, USDA, 2881 F & B Road, College Station, Texas 77845-2122

Received March 2, 1998

A comparison between three different methods commonly used to estimate ring current effects on chemical shifts is presented. Haigh–Mallion, Johnson–Bovey, and classical point-dipole approximations were used to estimate the ring current contribution to chemical shifts for protons in several proteins for which both detailed X-ray crystal structures and chemical shift assignments were available. For the classical point-dipole model, new proportionality constants were calculated by fitting to ring current estimations from both the quantum-mechanical Haigh–Mallion and semiclassical Johnson–Bovey methods and compared with the previously used point-dipole constant of Perkins and Dwek. Statistical analysis of the predictions obtained by all methods indicates that the point-dipole approximation parametrized against quantum-mechanical data is superior to the previously used classical model, comparable to Johnson–Bovey calculations, and slightly poorer than predictions from the Haigh–Mallion theory. The implementation of a pseudoenergy penalty term for use in structure refinement from chemical shift data based on the classical point-dipole model is described, and its usefulness in cases where other NMR information is limited is discussed with a specific example.

INTRODUCTION

NMR is one of the most important tools in three-dimensional structure determination of macromolecules in solution.^{1–3} Elegant new techniques and advances in instrumentation will extend the size barrier in the determination of protein and protein–DNA complexes structures beyond 30 KDa in the immediate future as well as increase the accuracy of these structures to levels presently reached only by X-ray crystallography.⁴ The main sources of structural information obtained from NMR experiments are internuclear distance constraints, derived from NOE experiments,^{1–3} and homo and hetero nuclear coupling constants, which can be used either to calculate dihedral angle constraints, or directly in structure refinement.^{1–3,5,6}

Chemical shifts have also been recognized as an important source of structural information.^{7,8} Although they are used mainly as a check on the accuracy of the calculated structures or to recognize regions of defined secondary structure in proteins,^{9,10} there are several studies of their direct incorporation in the refinement process.^{11–13} In peptides, the contributions to proton chemical shifts can be decomposed approximately into the following terms:^{14,15}

$$\sigma_{\text{observed}} \approx \sigma_{\text{calc}} = \sigma_{\text{random}} + \sigma_E + \sigma_{\text{ani}} + \sigma_{rc}$$

The first three terms include the random coil shift, electrostatic contributions from polar groups, and effects from the magnetic anisotropy of the peptide group, respectively. For an in depth analysis of the origins of these terms as well as other contributing factors to the observed proton chemical shift that are less often considered, the reader is directed to

the extensive literature available on the subject.^{15,16} The last term, σ_{rc} , quantifies the effects arising from aromatic ring currents and is the main focus of this report. Several textbooks and comprehensive reviews discuss the physical basis behind ring current effect calculations and discuss the different methods used to compute it.^{15,17} For a single aromatic ring, the mathematical expression used to calculate its effect over the shift of a proton in its vicinity has the general form

$$\sigma_{rc} = iBG(\mathbf{r})$$

where B is a general proportionality constant related to the magnetic susceptibility, i is the ring current intensity factor that varies according to the nature of the aromatic ring, and $G(\mathbf{r})$ is a spatial function expressed in cylindrical coordinates. The main difference among the commonly used ring current estimation methods is the form taken by $G(\mathbf{r})$. In the Haigh–Mallion theory, derived from quantum-mechanical calculations, this term takes the form¹⁸

$$G(\mathbf{r}) = \sum_{ij} S_{ij} (1/r_i^3 + 1/r_j^3)$$

where S_{ij} is the signed area of the triangle formed by the projection of the proton into the ring plane and atoms i and j of the ring, and r_i and r_j are the distances from atoms i and j to the proton, respectively. The summation is over all bonds of the aromatic ring. For the semiclassical Johnson–

Table 1. Protein Structures Used in the Calculations and Comparisons

entry ^a	protein	PDB code	resolution	assignments ^b
1	tendamistat	1HOE	2.00	245
2	human lysozyme	1LZ1	1.50	391
3	human ubiquitin	1UBQ	1.80	269
4	hen egg white lysozyme	2LZT	1.97	349
5	ribonuclease T1	2RNT	1.80	254
6	oxidized thioredoxin	2TRX	1.67	428
7	bacteriophage T4 lysozyme	3LZM	1.70	334
8	ribonuclease A	3RN3	1.45	341
9	turkey ovomucoid third domain	3SGB	1.80	172
10	bovine pancreatic trypsin inhibitor	5PTI	1.00	209
11	cutinase	1CEX	1.00	
12	crambin	1CRN	1.50	
13	reduced human thioredoxin	1ERT	1.70	
14	fatty acid binding protein	1IFC	1.20	
15	protein G third binding domain	1IGD	1.67	
16	subtilisin BL	1ST3	1.40	
17	endonuclease V	2END	1.45	
18	scorpion neurotoxin	2SN3	1.20	
19	bovine calbindin D-9k	5ICB	1.50	
20	bovine pancreatic trypsin inhibitor	6PTI	1.70	

^a All 20 structures were used in the reparametrization of the point-dipole model, while structures 1–10 were used for method comparisons.

^b References to NMR data for the 10 proteins can be found in ref 13.

Bovey theory, the geometric term has the following form:¹⁹

$$G(\mathbf{r}) = ((1 + \rho)^2 + z^2)^{-1/2} [K + (1 - \rho^2 - z^2)/((1 - \rho)^2 + z^2)E]$$

In this expression, ρ and z are the cylindrical coordinates of the proton for which the effect is being evaluated relative to the center of the aromatic ring, and K and E are the complete first and second elliptic integrals. $G(\mathbf{r})$ needs to be evaluated above and below the aromatic ring. Finally, the simplest method for calculating $G(\mathbf{r})$ is the classical point-dipole model of Pople²⁰

$$G(\mathbf{r}) = (1 - 3 \cos^2 \theta)/r^3$$

where θ is the angle between the normal to the plane of the aromatic ring passing through its center and the vector connecting the center of the ring to the observed proton, and r is the distance from the proton to the ring center.

The results obtained by these three methods are similar. The greatest discrepancies between them are found for protons situated very close to aromatic rings and for porphyrin macrocycles, where the point-dipole approximation greatly underestimates the shifts observed for protons lying directly above or below the macrocyclic ring.²¹ This model is therefore unsuitable for porphyrin containing proteins, but in view of its simplicity, ease of mathematical implementation, minimal computational requirements, and the preponderance of non-porphyrin containing proteins and peptides, it is surprising that most reports on direct use of proton chemical shifts in structure refinement instead utilized the Haigh–Mallion model to assess ring currents effects.^{10,11} The point-dipole approximation is perhaps viewed as too simplistic and unproven, as the only available comparisons between this and other methods were published by Perkins and Dwek nearly 20 years ago for small experimental data sets.²² In this report we present a more complete comparison between ring current models, a simple procedure for reparametrizing the classical point-dipole approximation and the implementation of this model into molecular modeling

calculations. We also present a specific example of its use in the structure determination of a small synthetic tripeptide for which conventional structure-related NMR information is very limited.

METHODS

Choice of Protein Chemical Shift Data and Structures.

For part of our study, proteins with published X-ray structures and proton chemical shift assignments were needed. Although the amount of NMR data for proteins has grown immensely in recent years, several data sets used in our analyses were taken from the original studies of Ösapay and Case,¹⁴ as they have also been used in other reports, allowing different results and methods to be compared.^{23,24} From the proteins used by Ösapay and Case, those with porphyrin groups were eliminated for the reasons discussed earlier as well as those in which the crystal structures were obtained with bound ligands. From the remaining 12 proteins, only those with resolutions of 2.0 Å or lower were considered as suggested by Szilágyi.⁸ This final set of 10 proteins had 896 Cα proton and 2096 side-chain proton resonance assignments, which compose the database used for comparing the different ring current models.

For the reparametrization of the point-dipole model, only X-ray data were needed, as discussed in the next section. Ten additional protein structures with resolutions below 1.8 Å were selected from the Protein Data Bank, giving a total of 20 structures that were used in the reparametrization procedure. A summary of the data for all the proteins used in our studies is presented in Table 1.

Reparametrization of the Classical Point-Dipole Model.

To date, parametrization of the different terms contributing to proton chemical shifts has usually been accomplished using experimental data.^{14,22–24} An analogous approach could be taken to calculate a new proportionality constant B for the point-dipole model using the much larger database of chemical shifts available. However, there are several drawbacks that have to be dealt with in such an approach. First, although it is commonly accepted that the structures

of globular proteins in solution and in the crystal are similar, it is not always the case. For example, there can be significant deviations between the NMR and X-ray structures for residues in the chain termini and at the protein surface.^{2,3,25} Another problem found in surface residue protons is the effects on the observed chemical shifts exerted by solvent molecules, which are not taken into account explicitly in shift calculation models. Finally, the protonation state of side-chains also needs to be considered, since it has a sizable effect on the chemical shift of protons close to the protonation site.¹⁴ All these and other factors may adversely affect the results, and thus careful analysis of the data used for parameter fitting is required.

To avoid these problems, a very simple procedure was devised. In a process resembling force field parameter derivation,²⁶ we used estimation methods with higher level of theory to calculate the proportionality constant B to be used in the classical point-dipole model. Since all models are estimations of the same effect, it is safe to assume that they are proportional to one another. Consistently, we can write

$$iB_{HM}G(\mathbf{r})_{HM} \propto iB_{JB}G(\mathbf{r})_{JB} \propto iB_{PD}G(\mathbf{r})_{PD}$$

Here B_{HM} , B_{JB} , $G(\mathbf{r})_{HM}$, and $G(\mathbf{r})_{JB}$ represent the Haigh–Mallion and Johnson–Bovey proportionality constants and spatial functions, respectively, and B_{PD} and $G(\mathbf{r})_{PD}$ are their counterparts in the point-dipole approximation. Although DFT calculations indicate that ring current intensity factors vary slightly for different ring current models,²⁷ the use of different i factors gives almost no variation in the accuracy of secondary shift estimations.²³ For this reason our calculations used the intensity factors reported by Ösapay and Case for all ring current models,¹⁴ which allows us to cancel them out from the above relationship:

$$B_{HM}G(\mathbf{r})_{HM} \propto B_{JB}G(\mathbf{r})_{JB} \propto B_{PD}G(\mathbf{r})_{PD}$$

The value of B_{PD} can now be easily calculated by a linear least-squares fit between the values obtained with the point-dipole spatial factor and ring current shifts obtained with either the quantum-mechanical or semiclassical models. A function of the form $y = k \cdot x$ was used in the regression analyses, since inclusion of an independent constant in the calculations has no physical basis, and showed no significant improvement on the quality of the fits. One advantage of this method is that, since the relationships are purely geometrical, the ring current effect contribution to chemical shift for *all protons in a structure* can be used in the parametrization. Even amides, which are normally not considered due to their large chemical shift dependence with pH and temperature, can be included in the calculations. As shown in Table 1, a total of 11 406 data points were obtained from the 20 protein structures selected and used in the re-estimation of the point-dipole proportionality constant B .

Implementation of the Model in Molecular Modeling Calculations. As normally done for other types of constraint information, chemical shifts can be introduced into molecular mechanic and dynamic calculations by means of a pseudoenergy penalty term, E_σ , which is added to the rest of the potentials present in the empirical force field.^{2,3,6,11} The penalty is usually a quadratic function, and for a single proton

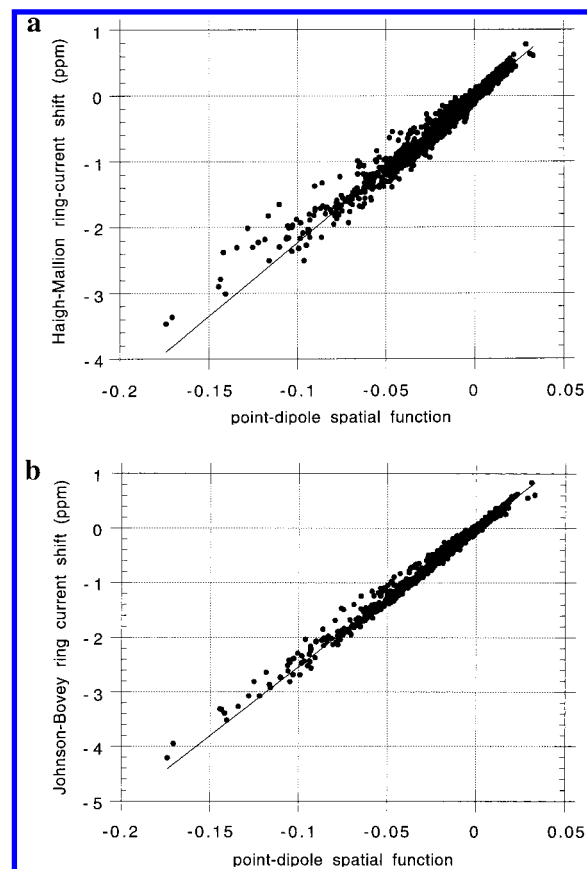


Figure 1. Correlation between the point-dipole spatial function and ring current contributions calculated by Haigh–Mallion (a) and Johnson–Bovey (b) models. A total of 11 406 points were used for the fits.

can be represented as

$$E_\sigma = K_\sigma (\sigma_{calc} - \sigma_{observed})^2$$

K_σ is a force constant, $\sigma_{observed}$ is the measured chemical shift, and σ_{calc} was defined earlier. The partial derivatives of this term with respect to the spatial coordinates of the atoms involved in the interaction have to be known to calculate the atomic forces acting during dynamic simulations and conjugate gradient minimizations. For example, if x_i is defined as the x coordinate of atom i , we have

$$\partial E_\sigma / \partial x_i = 2K_\sigma (\sigma_{calc} - \sigma_{observed}) * \partial \sigma_{calc} / \partial x_i$$

Substituting σ_{calc} by its definition and keeping in mind that both $\sigma_{observed}$ and σ_{random} are constants whose derivatives with respect to x_i are zero, we obtain

$$\partial E_\sigma / \partial x_i = 2K_\sigma (\sigma_{random} + \sigma_E + \sigma_{ani} + \sigma_{rc} - \sigma_{observed}) * (\partial \sigma_E / \partial x_i + \partial \sigma_{ani} / \partial x_i + \partial \sigma_{rc} / \partial x_i)$$

Since we are particularly interested in the ring currents effects, only the derivatives of this term will be considered below. Considering the polar variables r and θ present in the definition of the point-dipole approximation, the derivatives with respect to x_i can be calculated using the chain rule

$$\partial \sigma_{rc} / \partial x_i = (\partial \sigma_{rc} / \partial r) * (\partial r / \partial x_i) + (\partial \sigma_{rc} / \partial \theta) * (\partial \theta / \partial x_i)$$

Table 2. Results from the Reparametrization of the Point-Dipole Model

method ^a	<i>B</i> (ppm)	structures ^b	data points	<i>r</i>	<i>B</i> error (%)
Haigh–Mallion	21.82	1–10	5892	0.986	2.83
Johnson–Bovey	25.44	1–10	5892	0.997	0.64
Haigh–Mallion	22.34	1–20	11406	0.984	2.95
Johnson–Bovey	25.35	1–20	11406	0.996	0.78
Perkins and Dwek ^c	27.41				

^a Estimation method used to obtain data points for the fit to the point-dipole spatial function. ^b Protein structures from Table 1 used in the fits. ^c Proportionality constant from ref 21.

Substitution with the derivative of σ_{rc} with respect to r and θ yields the partial derivative with respect to x_i

$$\partial\sigma_{rc}/\partial x_i = 3iB_{PD}\{[(3\cos^2\theta - 1)/r^4]*(\partial r/\partial x_i) - (2\cos\theta\sin\theta/r^3)*(\partial\theta/\partial x_i)\}$$

The last step involves the conversion of polar to Cartesian coordinates and substitution of the derivatives of r and θ against x_i , which is straightforward since they are geometrically related. These calculations are long and beyond the scope of this report. In our case, most of the mathematical steps described above as well as those needed for implementing other terms responsible for secondary shifts were avoided using the Tripos Force Field Engine (FFE).²⁸ This programming environment allows the incorporation of new empirical potentials into the force field calculations without the need of explicitly defining the derivatives of the energy functions against Cartesian coordinates nor extensive modification of the program code housing the minimization and dynamics routines. Only the explicit function relating the energy with the Cartesian coordinates needs to be defined, making it ideal for the rapid implementation of novel force fields or the incorporation of potential energy terms to existing force fields. The code and instructions necessary for the setup of this pseudo energy term in Sybyl can be obtained freely from the authors.²⁹

General Considerations. NMR experiments were performed on a Bruker ARX-500 spectrometer operating at 500 MHz using an HCN probe. Samples were dissolved in H₂O–

D₂O (9:1), containing 3-(trimethylsilyl)propionic acid, sodium salt (TSP), as internal standard. 1D spectra were recorded with 32K data points and zero filled to 64K, while matrix sizes of 2K × 0.5K zero filled to 2K × 2K were used in 2D experiments. Presaturation was used for water signal suppression. A 600 ms high power pulsed spin lock was used for ROESY experiments.³⁰

Ring current contributions and chemical shift estimations based on Haigh–Mallion and Johnson–Bovey models were performed with the program SHIFTS (version 2.2),³¹ which was also used for all calculations of electrostatic and peptide group anisotropy contributions to chemical shifts. The program was modified to allow point-dipole approximation calculations, not implemented in the original code.³² Experimental chemical shifts for the proteins studied were kindly provided by Dr. David A. Case. All molecular modeling calculations were performed using SYBYL 6.3 (Tripos Associates Inc. St. Louis, MO) running on a Silicon Graphics Indigo R4000 workstation. The Weiner et al. force field and point charges were used for all molecular dynamics and mechanics simulations.^{33,34} A distance dependent dielectric constant ($\epsilon = R_{ij}$) and a nonbonded cutoff of 8 Å were used in all force field calculations. Additional parameters and charges needed to model the Fmoc protective group were obtained following a procedure previously reported by us.³⁵ The aromatic rings in the biphenyl system of the Fmoc group were treated independently for chemical shift contribution calculations in modeling experiments, using benzene ring current intensity factors (1.00).¹⁴ An energy gradient below 0.05 kcal/mol was employed as termination criteria in all energy minimizations. Force constants of 2.0 and 200 kcal/mol were used for the chemical shift and distance range pseudo energy terms, respectively. Comparison, superposition, and root-mean-square deviation (RMSD) calculation of structure sets was done with routines previously developed in our laboratory.³⁶

RESULTS

Point-Dipole Proportionality Constants. The results from the parametrization of the point-dipole model against quantum-mechanic and semiclassical calculations are sum-

Table 3. Statistics from Fits between Observed and Calculated Shifts Using Different Ring Current Models^a

proton set	<i>n</i>	point-dipole ^b									
		Haigh–Mallion		Johnson–Bovey		<i>B</i> _{H–M}		<i>B</i> _{J–B}		<i>B</i> _{P–D}	
		<i>r</i>	RMS	<i>r</i>	RMS	<i>r</i>	RMS	<i>r</i>	RMS	<i>r</i>	RMS
all	2992	0.854	0.220	0.846	0.228	0.846	0.226	0.844	0.229	0.841	0.235
H α	896	0.846	0.290	0.843	0.290	0.844	0.293	0.841	0.292	0.837	0.293
side-chain	2096	0.867	0.182	0.862	0.195	0.854	0.191	0.858	0.197	0.859	0.205
1HOE	245	0.833	0.237	0.818	0.268	0.823	0.248	0.813	0.278	0.807	0.299
1LZ1	391	0.866	0.226	0.850	0.247	0.851	0.234	0.847	0.246	0.845	0.256
1UBQ	269	0.811	0.195	0.806	0.198	0.807	0.198	0.805	0.199	0.803	0.200
2LZT	349	0.874	0.236	0.866	0.246	0.860	0.246	0.862	0.248	0.861	0.254
2RNT	254	0.920	0.211	0.916	0.217	0.917	0.233	0.915	0.226	0.910	0.222
2TRX	428	0.767	0.208	0.764	0.212	0.761	0.211	0.761	0.212	0.758	0.213
3LZM	334	0.840	0.219	0.835	0.221	0.845	0.219	0.840	0.219	0.836	0.211
3RN3	341	0.858	0.228	0.856	0.228	0.856	0.229	0.854	0.230	0.851	0.233
3SGB	172	0.826	0.214	0.835	0.214	0.835	0.208	0.841	0.209	0.844	0.214
5PTI	209	0.888	0.207	0.884	0.208	0.875	0.220	0.878	0.214	0.878	0.217

^a In all cases RMS indicates the root-mean-square error between observed and calculated shifts in ppm. ^b For the point-dipole model, *B*_{H–M} and *B*_{J–B} are proportionality constants from fits to Haigh–Mallion and Johnson–Bovey estimations, respectively, and *B*_{P–D} is the proportionality constant used by Perkins and Dwek.²¹

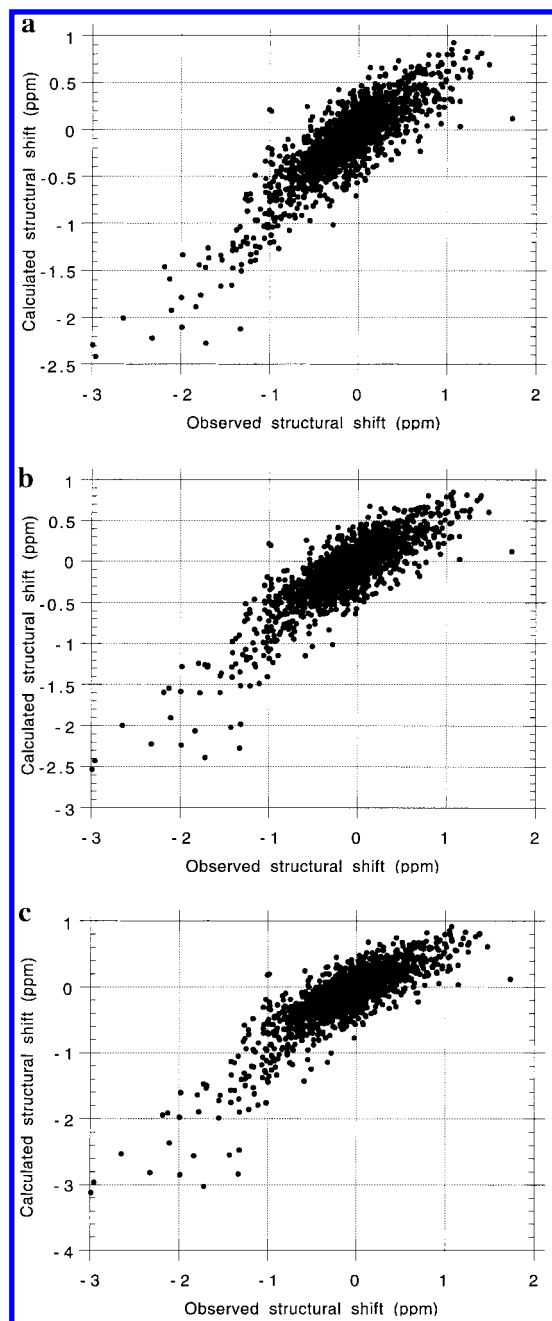


Figure 2. Correlation between observed chemical shifts and estimations using Haigh–Mallion (a) and point-dipole models with B constants from the reparametrization against Haigh–Mallion estimations (b) and from Perkins and Dwek (c).

marized in Table 2 and Figure 1. The quality of the fits is comparable in both cases. The slightly better fit obtained against results from the Johnson–Bovey model can be explained considering the symmetry of the spatial function $G(\mathbf{r})$ in the different models; in the point-dipole and Johnson–Bovey it has cylindrical symmetry, while in the Haigh–Mallion model it has hexagonal and pentagonal symmetry for six- and five-membered rings, respectively.^{17,21}

There are two aspects of the parametrization method that deserve attention. First, since only X-ray data were needed for the proposed procedure, the number of structures used to obtain B could be extended far beyond the 20 employed here. However, it was found that on increasing the number of data points used in the fits from 5892 to 11 406, which represents a doubling of the structures considered in the

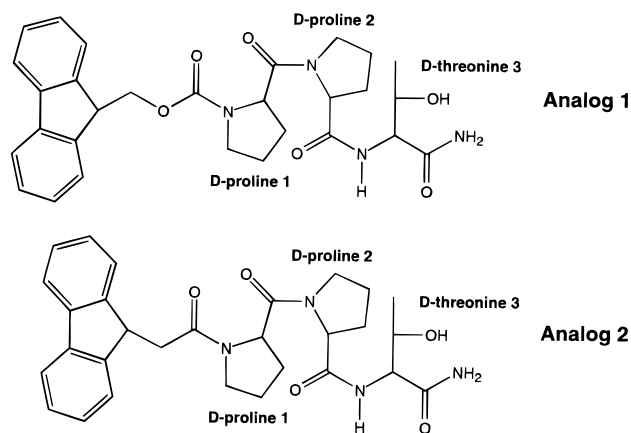


Figure 3. Chemical structure of D-amino acid tripeptide analogues 1 and 2 obtained from an insect kinin diuretic bioassay.

calculations, the results remained nearly constant. Changes of only 2.36% and 0.35% in the values of B were observed for fits against Haigh–Mallion and Johnson–Bovey estimations, respectively. These uncertainties are lower in each case than the errors of the calculated constants, reported in Table 2, and are thus within the accuracy limit of the parametrization method. Second, the two constants are slightly smaller than the one previously used by Perkins and Dwek, which was derived directly from χ_L , the magnetic susceptibility of benzene.³⁷ Although this can be viewed as a failure of the proposed method in reproducing the classical value of χ_L , the use of either of the constants obtained produces an overall improvement in the estimation of chemical shifts for the proteins analyzed in this study, as discussed in detail in the following section.

Comparison of Ring Current Models. Table 3 and Figure 2 summarize the results from the evaluations of the different ring current models against experimental data. The previously reported similarity in predictions among different methods is corroborated in our results, but there are differences from earlier studies. The original comparisons of Perkins and Dwek were performed on a database of only 76 experimental resonances, consisting mainly of methyl group and aromatic protons of lysozyme, and relied only on ring current estimations to calculate chemical shifts.²² More recent method comparisons by Williamson and Asakura used a total of 768 assignments for their analyses but did not consider the point-dipole model.²⁴ The present study uses a much larger database, with a total of 2992 experimental chemical shifts. Peptide group anisotropy and electrostatic effects, which have been shown to greatly improve the quality and predictive power of chemical shift calculations,¹⁴ were also utilized in our calculations.

When considering all protons in the database, the accuracy of Haigh–Mallion, Johnson–Bovey, and the earlier point-dipole model estimations decreases in that order, following the same trend reported in the literature. However, there is an improvement in accuracy for point-dipole model predictions when the new constants are used. Although small, it was not only found when analyzing the entire data set, but for most of the individual entries as well, as indicated in Table 3. A clear exception is turkey ovomucoid third domain (3SGB), in which there is an apparent reversal of accuracy among the different methods. In this case, the NMR measurements were performed on the isolated protein,³⁸ while

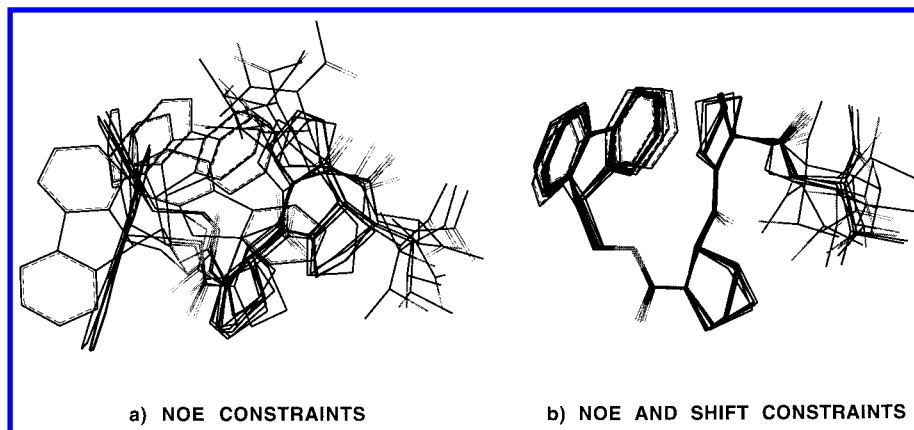


Figure 4. Backbone atom superposition of 10 low energy conformations obtained from the conformational search for analogue **1** without (a) and with (b) the inclusion of chemical shift constraints. Hydrogens omitted for clarity.

the crystal structure was obtained as a complex with *Streptomyces griseus* protease B.³⁹ Differences between the X-ray and solution structures are more likely in this situation and could account for the inconsistencies observed. Of the two new *B* proportionality constants, the one obtained in the parametrization against quantum-mechanical estimations gave the best results, with an increase in the Pearson's *r* correlation coefficient from 0.841 to 0.846 and a decrease in the prediction RMS errors from 0.235 to 0.226 ppm. It is worth noting that when this constant was used, classical point-dipole and Johnson–Bovey estimations were statistically identical. For predictions using the constant obtained from semiclassical estimations, the *r* coefficient was 0.844 and the RMS error dropped to 0.229 ppm.

A similar tendency is observed when the chemical shift data for C α protons were analyzed. An improvement in accuracy for point-dipole predictions is also found when either of the two new proportionality constants are used. Again, the *B* constant obtained from Haigh–Mallion estimations gave the best results, with an increase of the *r* correlation coefficient from 0.837 to 0.844 and equal prediction RMS errors. For these protons, the use of this new constant gives the point-dipole model almost the same accuracy in calculations as that of the quantum-mechanically derived method, at a fraction of the computational cost.

Slightly poorer results were found for side-chain protons. Both Haigh–Mallion and Johnson–Bovey estimations are superior to point-dipole estimations, independently of the proportionality constant used. Among these, there appears to be no gain in accuracy for calculations with the new *B* constants derived here. There is, however, a decrease in the RMS error for the predictions with either of them, the lowest being obtained with the constant parametrized from Haigh–Mallion calculations.

Overall, the use of the point-dipole model with a proportionality constant derived from Haigh–Mallion estimations gives the best results for the classical ring current model, and for C α protons the estimations were statistically equal to methods with higher level of theory. The biggest discrepancies were found for side-chain protons, particularly in cases where the deviations from the random coil chemical shifts were higher than 1.0 ppm. It has been shown that side-chain proton secondary shifts can be estimated more accurately using ring current models alone,^{13,21} indicating that this type of effect governs departures from random coil

values in these cases. Large deviations in side-chain proton shifts would then indicate close proximity to aromatic rings, and our results merely reflect the fact that the point-dipole model has poorer predictive ability in these conditions.

Solution Structure of Fmoc-dPro-dPro-dThr-NH₂. To assess the significance of considering chemical shift data in structure determination and the usefulness of the point dipole model estimation of ring current effects in molecular modeling, the conformation of a small tripeptide was studied both with and without the inclusion of this information. The test molecule, Fmoc-dPro-dPro-dThr-NH₂ (**1**, Figure 3), is a synthetic analogue selected from a large combinatorial library of tripeptides containing D-amino acids by means of on an insect kinin bioassay in which stimulation of malpighian tubule secretion is monitored.⁴⁰ Due in part to the small amount of material available for NMR analysis, the information obtained from ROESY spectra correlations was limited to intraresidue and sequential interproton distances. However, the peaks of one of the C δ protons⁴¹ and the C α proton of D-proline-2 were shifted upfield 0.9 and 0.6 ppm, respectively, from their random coil values. This was qualitatively interpreted as a folding of the Fmoc protective group toward the tripeptide in a manner that would maximize favorable packing of the aromatic rings and the D-proline side-chain,⁴² placing the aromatic rings above the aforementioned protons. Further support for this assumption came from NMR data of the related analogue **2**, shown in Figure 3. This synthetic neuropeptide has similar chemical structure, differing only in a shorter connecting segment between the protective group and the tripeptide which makes the folded conformation of compound **1** unlikely. Both compounds are equipotent in biological assays,⁴⁰ indicating that only the peptidic portion of the molecules is responsible for activity. The chemical shifts for the protons in **2** show no substantial deviations from random coil values. From these observations it was assumed that the deviations from random coil values observed in the proton resonances of tripeptide **1** were mainly due to ring current effects, making it suitable for our purposes.

The conformational search for the tripeptide with and without the inclusion of chemical shift constraints was done in identical conditions and is briefly described here. Four different starting conformations were generated by distance geometry, and each of them was used in 100 cycles of simulated annealing experiments,⁴³ consisting of heating at

1000 K for 1 ps, exponential annealing to 200 K for 1 ps, followed by energy minimization. The 10 conformers with the lowest energy from the four experiments were used for structure analysis. Superpositions of the two sets of structures generated with this protocol are shown in Figure 4.

The energies of the structures for the set obtained in the absence of chemical shift data were within 2.98 kcal/mol of the ensemble minimum, which was 4.68 kcal/mol. The RMSD for the backbone atoms is 1.2 Å, indicating a sizable dispersion of the structures in space. The presence of different conformational families of similar energy in which the peptide bonds are either in *cis* or *trans* configuration is also evident from the figure. Finally, only a few of the structures obtained would explain the abnormal chemical shifts observed experimentally.

On the other hand, the structure set obtained through modeling including secondary shift constraints had an RMSD of only 0.2 Å and consisted of a single family of conformers in which both peptide bonds were in *trans* configuration. Although an increase in the relative energy for the structures in this set can be expected upon the inclusion of the chemical shift penalty term, the energies of the conformers in the ensemble were within 3.90 kcal/mol from the minimum of 5.80 kcal/mol, only slightly higher than in the set obtained when no additional penalty terms were used. This indicates that the incorporation of chemical shift information during dynamics and energy minimization only guides the conformational search toward one of the low energy forms available to the molecule, greatly reducing the computing time needed to obtain structures consistent with the experimental NMR data. The structure obtained for the tripeptide is also in accordance with the proposed conformation of the insect kinin active core, showing a turn in the peptidic region that would mimic the β -turn presumed to be critical for activity in the natural neuropeptide.⁴⁴

DISCUSSION

The method for parametrization of the classical point-dipole model presented here provides a simple and accurate route for the estimation of the proportionality constant *B* from models with a higher level of theory. It thus eliminates the need of obtaining a vast number of experimental protein chemical shift assignments for use in the parametrization, making it comparable to force field parametrization against *ab initio* or semiempirical data. The results obtained using the new constants found by this procedure show an improvement over the previously used point-dipole approximation, indicating that it is indeed a reasonable approach for reparametrizing this ring current model. Only the *B* proportionality constant was recalculated in our case, while intensity factors for all aromatic rings were considered constant and equal to those reported earlier. A small improvement can be expected if these factors are also considered as variable parameters in the regression analyses, using the recently reported intensity factors for Haigh–Mallion and Johnson–Bovey models.²⁷ Studies along this line are presently underway.

The comparisons between the different ring current models presented not only confirm the similarity in their predictions but also indicate that their accuracy is comparable. This is especially true when the new proportionality constants are

employed for the point-dipole model, in which case it has similar levels of accuracy to semiclassical methods. This accuracy, together with its mathematical simplicity, makes the point-dipole model suitable for use in structure determination from NMR data. A method that allows for a thorough search of the conformational space available to the molecule and the generation of a large ensemble of structures consistent with the NMR data without imposing steep computational requirements is desirable in the initial stages of the molecular modeling calculations. Some exceptions do have to be considered, such as porphyrin containing proteins and protons with large deviations from random coil shifts, where the accuracy of the point-dipole model is known to decline.

Although there are a number of reports on the impact of proton chemical shift constraints in structure refinement, extensive interproton distance information was available in these cases.^{10,11} In our study of neuropeptide **1**, the information from NOE interactions is not sufficient to establish the conformation of this compound in solution, making the inclusion of chemical shift information of vital importance. There is a remarkable improvement in the results obtained with the incorporation of only two secondary shift constraints, making chemical shifts and the simple point-dipole model for ring current effects invaluable tools for the structural studies of small peptides in solution. Further studies on similar tripeptides in which similar abnormal deviations from random coil shifts are observed are currently underway. The results of these investigations and their implications on the structure–activity relationships of synthetic kinins will be reported elsewhere.

ACKNOWLEDGMENT

The authors wish to acknowledge the NIH for financial aid. Financial support from the NFS through Grant CHE-9528196 is also acknowledged. We also thank Dr. Dave A. Case for providing us with the files containing experimental chemical shifts data and important suggestions concerning the ring current method comparisons.

REFERENCES AND NOTES

- (1) Wüthrich, K. *NMR of Proteins and Nucleic Acids*; Wiley & Sons: New York, 1986.
- (2) Williamson, M. P. NMR of proteins. *Nat. Prod. Rep.* **1993**, *10*, 207–232.
- (3) Evans, J. N. S. *Biomolecular NMR Spectroscopy*; Oxford University Press: New York, 1995.
- (4) Tjandra, N.; Bax, A. Direct measurement of distances and angles in biomolecules by NMR in a dilute liquid crystalline medium. *Science* **1997**, *278*, 1111–1114.
- (5) Mierke, D. F.; Kessler, H. Combined use of homo- and heteronuclear coupling constants as restraints in molecular dynamic simulations. *Biopolymers* **1992**, *32*, 1277–1282.
- (6) Garret, D. S.; Kuszewski, J.; Hancock, T. J.; Lodi, P. J.; Vuister, G. W.; Gronenborn, A. M.; Clore, G. M. The impact of direct refinement against three-bond HN–C α H coupling constants on protein structure determination by NMR. *J. Magn. Reson. B* **1994**, *104*, 99–103.
- (7) Bundi, A.; Wüthrich, K. ¹H NMR parameters of the common amino acid residues measured in aqueous solution of the linear tetrapeptide H-Gly-Gly-X-L-Ala-OH. *Biopolymers* **1979**, *18*, 285–297.
- (8) Szilágyi, L. Chemical shifts in proteins come of age. *Prog. NMR Spectrosc.* **1995**, *27*, 325–443.
- (9) Wishart, D. S.; Sykes, B. D.; Richards, F. M. The chemical shift index: A fast and simple method for the assignment of protein secondary structure through NMR spectroscopy. *Biochemistry* **1992**, *31*, 1647–1651.

- (10) Williamson, M. P.; Kikuchi, J.; Asakura, T. Application of ^1H NMR chemical shifts to measure the quality of protein structures. *J. Mol. Biol.* **1995**, *247*, 541–546.
- (11) Kuszewski, J.; Gronenborn, A. M.; Clore, G. M. The impact of direct refinements against protons chemical shifts on protein structure determination by NMR. *J. Magn. Reson. B* **1995**, *107*, 293–297.
- (12) Ösapay, K.; Theriault, Y.; Wright, P. E.; Case, D. A. Solution structure of carbonmonoxy myoglobin determined from NMR distance and chemical shift constraints. *J. Mol. Biol.* **1994**, *244*, 183–197.
- (13) Kuszewski, J.; Qin, J.; Gronenborn, A. M.; Clore, G. M. The impact of direct refinement against $^{13}\text{C}\alpha$ and $^{13}\text{C}\beta$ chemical shifts on protein determination by NMR. *J. Magn. Reson. B* **1995**, *106*, 92–96.
- (14) Ösapay, K.; Case, D. A new analysis of proton chemical shifts in proteins. *J. Am. Chem. Soc.* **1991**, *113*, 9436–9444.
- (15) Harris, R. K. *Nuclear Magnetic Resonance Spectroscopy, A Physicochemical View*; Longman, Scientific & Technical: Essex, England, 1986.
- (16) Williamson, M. P.; Asakura, T. Protein Chemical Shifts. In *Methods in Molecular Biology. Protein NMR Techniques*; Reid, D. G., Ed.; Humana Press: Totowa, NJ, 1997; Vol. 60, Chapter 3.
- (17) Haigh, C. W.; Mallion, R. B. Ring current theories in nuclear magnetic resonance. *Prog. NMR Spectrosc.* **1980**, *13*, 303–344.
- (18) Haigh, C. W.; Mallion, R. B. Proton magnetic resonance of nonplanar condensed benzenoid hydrocarbons II. Theory of chemical shifts. *Mol. Phys.* **1971**, *22*, 955–970.
- (19) Johnson, C. E.; Bovey, F. A. Calculation of nuclear magnetic resonance spectra of aromatic hydrocarbons. *J. Chem. Phys.* **1958**, *29*, 1012–1014.
- (20) Pople, J. A. Proton magnetic resonance of hydrocarbons. *J. Chem. Phys.* **1956**, *24*, 1111.
- (21) Perkins, S. J. Application of ring current calculations to proton NMR of proteins and transfer RNA. In *Biological Magnetic Resonance*. Berliner, L. J., Reuben, J., Eds.; Plenum Press: New York, 1982; Vol. 4, Chapter 4.
- (22) Perkins, S. J.; Dwek, R. A. Comparisons of ring-current shifts calculated from the crystal structure of egg white lysozyme of hen with the proton nuclear magnetic resonance spectrum of lysozyme in solution. *Biochemistry* **1980**, *19*, 245–258.
- (23) Williamson, M. P.; Asakura, T. Calculation of chemical shifts of protons on alfa carbons in proteins. *J. Magn. Reson.* **1991**, *94*, 557–562.
- (24) Williamson, M. P.; Asakura, T. Empirical comparisons of models for chemical-shift calculations in proteins. *J. Magn. Reson. B* **1992**, *101*, 63–71.
- (25) Wüthrich, K. Six years of protein structure determination by NMR spectroscopy: what have we learned? In *Protein Conformation. Ciba Foundation Symposium 161*; John Wiley & Sons: Chichester, 1991; pp 136–149.
- (26) Hopfinger, A. J.; Pearlstein, R. A. Molecular mechanics force-field parametrization procedures. *J. Comput. Chem.* **1984**, *5*, 486–499.
- (27) Case, D. Calibration of ring-current effects in proteins and nucleic acids. *J. Mol. Biol.* **1995**, *6*, 341–346.
- (28) *Sybyl 6.3 Force Field Engine Manual*; Tripos Associates, Inc.: St. Louis, MO, 1995.
- (29) The programs are distributed by request to gmoyna@cbnmr.chem.tamu.edu.
- (30) Kessler, H.; Griesinger, C.; Kerssebaum, R.; Wagner, K.; Ernst, R. R.; Separation of cross-relaxation and J cross-peaks in 2D rotating-frame NMR spectroscopy. *J. Am. Chem. Soc.* **1987**, *109*, 607–609.
- (31) SHIFTS 2.2 was obtained at <http://www.scripps.edu/case/casegroup.html>.
- (32) A copy of the modified SHIFTS code used to compute chemical shifts with the point-dipole model can be obtained from the authors.
- (33) Weiner, S. J.; Kollman, P. A.; Case, D. A.; Singh, U. C.; Ghio, C.; Alagona, G.; Profeta, S.; Weiner, P. A new force field for molecular mechanical simulations of nucleic acids and proteins. *J. Am. Chem. Soc.* **1984**, *106*, 765–784.
- (34) Weiner, S. J.; Kollman, P. A.; Nguyen, D. T.; Case, D. A. An all atom force field for simulations of proteins and nucleic acids. *J. Comput. Chem.* **1986**, *7*, 230–252.
- (35) Moyna, G.; Hernandez, H.; Williams, H. J.; Nachman, R. J.; Scott, A. I. Development of Weiner et al. force field parameters suitable for conformational studies of [1,4]-benzodiazepines and related compounds. *J. Chem. Inf. Comput. Sci.* **1997**, *37*, 951–956.
- (36) Moyna, G.; Mediawala, S.; Williams, H. J.; Scott, A. I. A simple algorithm for superimposing sets of NMR derived structures: Its application to the conformational study of cephalomarine in lipophobic and lipophilic solution. *J. Chem. Inf. Comput. Sci.* **1996**, *36*, 1224–1227.
- (37) Pauling, L. The diamagnetic anisotropy of aromatic molecules. *J. Chem. Phys.* **1936**, *4*, 673–677.
- (38) Robertson, A. D.; Westler, W. M.; Markley, J. L. Two-dimensional NMR studies of Kazal proteinase inhibitors. 1. Sequence-specific assignments and secondary structure of turkey ovomucoid third domain. *Biochemistry* **1988**, *27*, 2519–2529.
- (39) Read, R. J.; Fujinaga, M.; Sielecki, A. R.; James, M. N. G. Structure of the complex of *Streptomyces griseus* protease B and the third domain of the turkey ovomucoid inhibitor at 1.8 Å resolution. *Biochemistry* **1983**, *22*, 4420.
- (40) Coast, G. M.; Holman, M. G.; Nachman, R. J. The diuretic activity of a series of cephalomyotropic neuropeptides, the acetakinins, on isolated malpighian tubules of the house cricket, *Acheta domestica*. *J. Insect Physiol.* **1990**, *36*, 481–488.
- (41) The ROESY spectrum indicates that the C δ proton showing deviation from random coil values lies on the same side of the D-proline ring as the C α proton.
- (42) Demchuk, E.; Bashford, D.; Gippert, G. P.; Case, D. Thermodynamics of a reverse turn motif. Solvent effects and side-chain packing. *J. Mol. Biol.* **1997**, *270*, 305–317.
- (43) Nigles, M.; Clore, G. M.; Gronenborn, A. M. Determination of three-dimensional structures of proteins from interproton distance data by hybrid distance geometry-dynamical simulated annealing calculations. *FEBS Lett.* **1988**, *229*, 317–324.
- (44) Roberts, V. A.; Nachman, R. J.; Coast, G. M.; Hariharan, M.; Chung, J. S.; Holman, M. G.; Williams, H. J.; Tainer, J. A. Consensus chemistry and β -turn conformation of the active core of the insect kinin neuropeptide family. *Chem. Biol.* **1997**, *4*, 105–117.

CI980402E